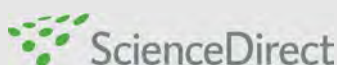
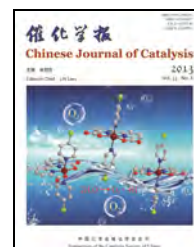


available at www.sciencedirect.comjournal homepage: www.elsevier.com/locate/chnjc

Article

Temperature-programmed desorption and surface reaction studies of CO on Co₂C

Yanpeng Pei^{a,c}, Yunjie Ding^{a,b,*}, Juan Zang^{a,c}, Xiangen Song^{a,c}, Wenda Dong^{a,c}, Hejun Zhu^a, Tao Wang^a, Weimiao Chen^a^a Dalian National Laboratory for Clean Energy, Dalian Institute of Chemical Physics, Chinese Academy of Sciences, Dalian 116023, Liaoning, China^b State Key Laboratory for Catalysis, Dalian Institute of Chemical Physics, Chinese Academy of Sciences, Dalian 116023, Liaoning, China^c University of Chinese Academy of Sciences, Beijing 100049, China

ARTICLE INFO

Article history:

Received 7 April 2013

Accepted 10 May 2013

Published 20 August 2013

Keywords:

Cobalt carbide

Passivation layer

Carbon monoxide adsorption

Hydrogenation

Alcohol

ABSTRACT

Cobalt carbide (Co₂C) samples were prepared by carburizing Co with CO at 473 K for in excess of 400 h and were characterized by X-ray diffraction, transmission electron microscopy, CO temperature-programmed reduction, CO temperature-programmed desorption (CO-TPD), and CO temperature-programmed surface reaction. The prepared Co₂C samples were composed of bulk Co₂C with a surface CoO passivation layer. The passivation layer could be removed by reaction with CO at 477 K. CO desorbing at low temperature in CO-TPD experiments likely originated from chemisorbed CO. CO desorbing at high temperature was likely due to residual CO within the Co₂C crystal lattice. CO adsorbed on Co₂C reacted with H₂ to form alcohol.

© 2013, Dalian Institute of Chemical Physics, Chinese Academy of Sciences.

Published by Elsevier B.V. All rights reserved.

1. Introduction

Transition metal carbides behave similarly to noble metals in heterogeneous catalysis and have received much attention since the first report by Levy and Boudart [1]. They exhibit outstanding performance in hydrogenation [2], ammonia synthesis [3], hydrodesulfurization [4], hydrodenitrogenation [5], water-gas shift reaction [6], hydrocarbon isomerization [7], and methane reforming [8]. However, few literatures were reported about the fundamental studies on the properties of transitional metal carbide catalysts. This is particularly so for cobalt carbide (Co₂C), whose formation is regarded as a deactivation sign of Fischer-Tropsch catalysts [9,10]. Ding et al. [11,12] recently reported that the generation of C₁–C₁₈ linear alcohols over activated carbon-supported Co catalysts could occur via the formation of Co₂C. The presence of Li or La tuned

the formation of Co₂C and thus influenced the selectivity of the alcohols [13–16].

CO temperature-programmed desorption (CO-TPD) and CO temperature-programmed surface reaction (CO-TPSR) are widely used surface sensitive techniques. They can provide information about CO adsorption and the reaction mechanism of different catalyst systems [17]. Volkov et al. [18] suggested that Co₂C could adsorb CO without rupture, in such a way that formed alcohols. To our knowledge, the adsorption properties of CO on Co₂C have not yet been reported. Optical spectroscopy is of limited use in investigating CO adsorption on Co₂C because Co₂C is opaque in the infrared region. The adsorption and reaction of CO on Co₂C can be investigated using CO-TPD and CO-TPSR, to better understand its catalytic behavior.

Herein, Co₂C was prepared according to the literature [19] and characterized by physical and chemical methods. CO ad-

* Corresponding author. Tel/Fax: +86-411-84379143; E-mail: djy@dicp.ac.cn

sorption and reaction on Co_2C were then investigated using CO-TPD and CO-TPSR.

2. Experimental

2.1. Co_2C preparation

Co_3O_4 (10.0 g) was reduced in flowing H_2 (60 ml/min) at 523 K for 4 h and then carburized in flowing CO (60 ml/min) at 493 K. Samples carburized for 468 and 605 h were denoted Co_2C -A and Co_2C -B, respectively, and were investigated for comparison. After reaction, samples were quenched to room temperature under Ar and then passivated in flowing 1 vol% O_2/Ar (60 ml/min) for 2 h before exposure to the atmosphere.

2.2. Characterization

X-ray diffraction (XRD) analysis was performed on a PANalytical X'Pert PRO diffractometer, using Cu $K_{\alpha 1}$ radiation at an operating voltage and current of 40 kV and 40 mA, respectively. The scan range was $2\theta = 20^\circ$ – 60° , and scan speed was $6^\circ/\text{min}$.

High resolution transmission electron microscopy (HRTEM) measurements were carried out using a FEI Tecnai G2 F30 microscope at an accelerating voltage of 300 kV.

CO-temperature-programmed reduction (CO-TPR) was carried out using a Micromeritics Autochem 2910 apparatus. A 200 mg sample was treated in flowing CO (20 ml/min), and the reduction temperature was increased from room temperature to 573 K at a rate of 5 K/min. CO consumption and CO_2 generation were recorded with an Omnistar 300 quadrupole mass spectrometer.

CO-TPD was carried out on the same instrument. A 200 mg sample was used for each test. The samples were first pre-reduced in-situ in flowing CO, and the temperature was raised from room temperature to 523 K at a rate of 5 K/min and maintained there for 1 h. Samples were purged with He at 523 K for 0.5 h, cooled to 323 K under flowing He, and purged with He for a further 40 min to remove adsorbed species. CO was pulsed over pre-treated Co_2C samples at 323 K until the TCD signal reached a constant value. Samples were flushed with He for 10 min, and the temperature linearly increased from 323 to 1173 K at 5 K/min under flowing He. The CO-TPD result of a 200 mg Co_2C -A sample under He was used as a blank experiment. Desorbed exit-gases were analyzed with an Omnistar 300 quadrupole mass spectrometer.

CO-TPSR was carried out on the same instrument. Sample (200 mg) was pre-reduced in flowing CO at 523 K for 1 h, purged with He at 523 K for 30 min, and cooled to 323 K. CO adsorption was carried out at 323 K by pulsing CO until the TCD signal reached a constant value. Samples were flushed with He for 10 min, and 10% H_2/Ar was allowed to flow through the sample bed. The temperature was increased to 1000 K at 5 K/min, and mass spectrometry was used for detection.

3. Results and discussion

3.1. XRD and TEM

Figure 1 shows XRD patterns of Co_2C -A and Co_2C -B. Both samples exhibit five identical diffraction peaks at $2\theta = 37.0^\circ$, 41.3° , 42.5° , 45.7° , and 56.6° , ascribed to the characteristic peaks of Co_2C (PDF 01-072-1369). No peaks of Co or CoO are observed, indicating that the bulk sample phase was Co_2C .

Figure 2 shows representative HRTEM images of Co_2C -A. Figure 2(a) shows a lattice spacing of 2.16 Å, ascribed to the (111) plane of Co_2C (PDF 01-072-1369). The lattice spacing of 2.46 Å in Fig. 2(b) is ascribed to the (111) plane of CoO (PDF 00-009-0402). Combined with XRD results, it suggests that samples were composed of bulk Co_2C with a surface CoO passivation layer.

3.2. CO-TPR

The passivation layer is reported to impact on the adsorption and reaction behavior of transitional metal carbides, and is typically removed before reaction [20,21]. The reduction behavior of the passivation layer of Co_2C -A was investigated by CO-TPD, as shown in Fig. 3. The CO consumption peak is at 477 K, and a CO_2 peak was simultaneously generated. This suggests that the passivation layer may have been reduced by the presence of CO.

3.3. CO-TPD

Figure 4(a) shows CO-TPD profiles of Co_2C -A and Co_2C -B, in which there exist two peaks for each sample. Peaks of Co_2C -A

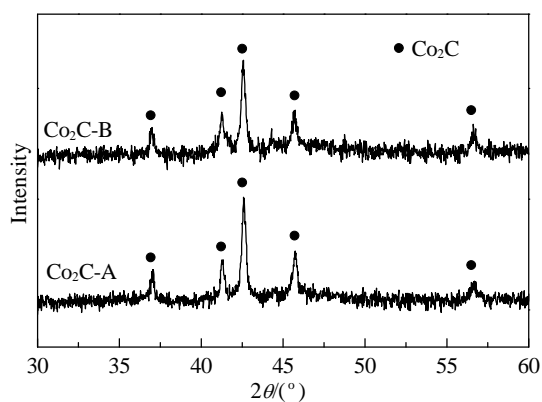


Fig. 1. XRD patterns of Co_2C samples.

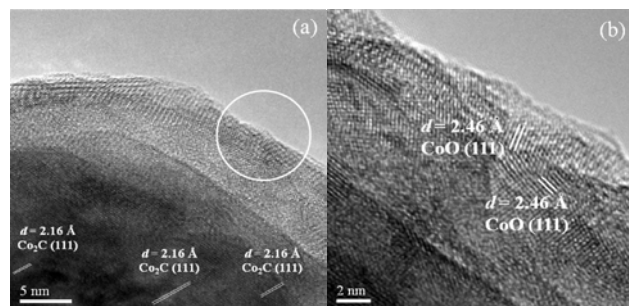


Fig. 2. HRTEM images of Co_2C -A. The circled region in (a) is shown at higher magnification in (b).

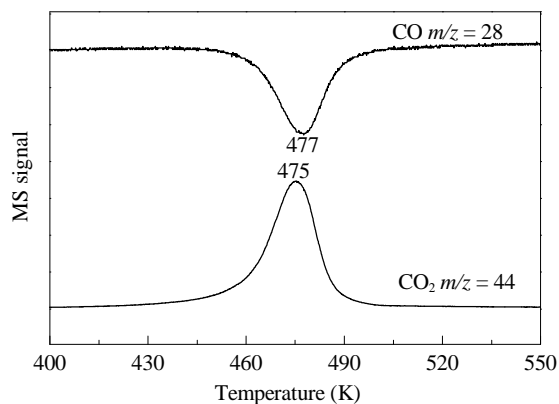


Fig. 3. CO-TPR profiles of Co₂C-A sample.

and Co₂C-B at lower temperature are denoted as A_L and B_L, respectively, and those at higher temperature as A_H and B_H, respectively. The peak temperatures of A_L and B_L are identical, but that of A_H is higher than B_H. The peak areas of A_L and A_H are smaller than those of B_L and B_H, respectively. Co₂C has been reported to slowly decompose above 573 K, but this process should be accelerated at 632 K [22]. A_L and B_L can be reasonably assigned to CO desorbed from Co₂C sites. A_H and B_H probably originate from other species after Co₂C decomposition. C source molecules are likely to remain in the metal carbide lattice after preparation as undissociated/dissociated molecules, similarly to nitrogen source molecules in metal nitrides [23,24]. Figure 4(a) shows that the lattice C content probably approaches the maximum value of 9.24%, as carburization time progresses. This results in increased active sites for CO adsorption on the Co₂C surface. Prolonged carburization results in more active sites, and more residual CO in the Co₂C lattice. Differing peak temperatures of A_H and B_H indicate that the lattice C content probably also impacted on the desorption temperature of residual CO.

An additional CO-TPD experiment investigating species desorbed from Co₂C-A without dosing under inert gas was used as a blank test. The result is shown in Fig. 4(b). The peak at 768 K

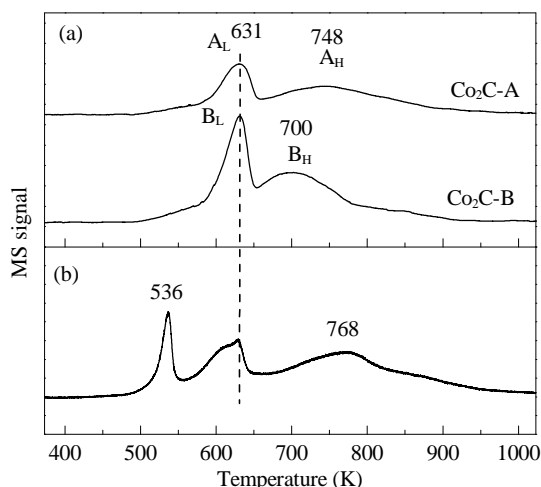


Fig. 4. CO-TPD profiles of the Co₂C samples (a) and the Co₂C-A without dosing (b).

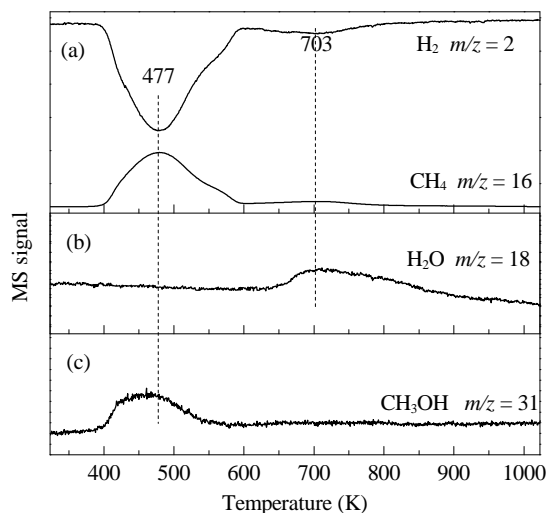


Fig. 5. CO-TPSR profiles of adsorbed CO on Co₂C.

coincides with A_H and B_H. As mentioned above, Co₂C is unstable at high temperature, suggesting that the species desorbed at this temperature was likely to be residual CO from the bulk Co₂C lattice. The peak centered at 631 K is still present and correlates well with A_L and B_L. This suggests that CO remained on Co₂C samples following synthesis [23]. A new peak appeared at 536 K, indicating that the desorbed species probably originated from the passivation layer of Co₂C-A because this sample was not reduced.

3.4. CO-TPSR

Figure 5 shows CO-TPSR profiles of adsorbed CO on Co₂C-A. Two H₂ ($m/z = 2$) consumption peaks at 477 and 703 K, and two CH₄ ($m/z = 16$) peaks at corresponding temperature are observed, as shown in Fig. 5(a). The CH₄ peak at 477 K is thought to be due to decomposition of Co₂C, according to the literature [19,25]. The CH₄ peak at 703 K arises from the hydrogenation of residual CO from the bulk Co₂C lattice. Figure 5(b) shows that H₂O ($m/z = 18$) was only observed at 703 K, which supports our above suggestion. Figure 5(c) shows that a methanol ($m/z = 31$) signal appeared as Co₂C decomposed. This is attributed to CO adsorbed on the Co₂C surface being hydrogenated into methanol. The CH₄ peak temperature on TPSR spectra generally closely corresponds with the CO dissociation ability of conventional cobalt based catalysts [14,26]. The CH₄ peak at low temperature is due to the decomposition of Co₂C rather than hydrogenation of adsorbed CO. We propose that the hydrogenation of CO adsorbed on Co₂C was responsible for the formation of methanol.

4. Conclusions

Co₂C was synthesized according to a reported method and physically and chemically characterized. The adsorption and reaction of CO on Co₂C was investigated. The Co₂C samples were composed of a bulk Co₂C phase and a surface CoO passivation layer. The later could be reduced by CO at 477 K. CO

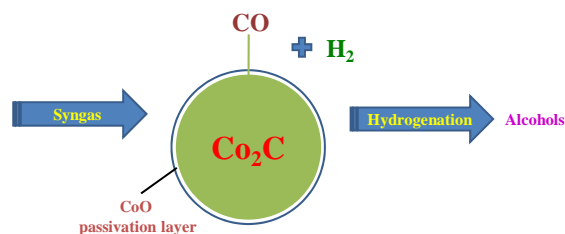
Graphical Abstract

Chin. J. Catal., 2013, 34: 1570–1575 doi: 10.1016/S1872-2067(12)60615-9

Temperature-programmed desorption and surface reaction studies of CO on Co₂C

Yanpeng Pei, Yunjie Ding*, Juan Zang, Xiangen Song, Wenda Dong, Hejun Zhu, Tao Wang, Weimiao Chen
Dalian Institute of Chemical Physics, Chinese Academy of Sciences;
University of Chinese Academy of Sciences

Co₂C was prepared by carburizing Co with CO. The prepared Co₂C samples were composed of a bulk Co₂C phase and an outer CoO passivation layer. Co₂C could adsorb CO, which was hydrogenated into alcohol.



could be adsorbed on Co₂C and was subsequently converted into alcohol via hydrogenation. The possibility of methanol forming at Co sites could not be excluded. However, the adsorption and reaction of CO on isolated Co₂C samples suggested that Co₂C was the active site for forming alcohol on supported Co catalysts. Unsupported Co₂C has potential in catalytic materials for alcohol synthesis from syngas. Further investigation of the role that Co₂C plays in alcohol formation is in progress.

References

- [1] Levy R B, Boudart M. *Science*, 1973, 181: 547
- [2] Oyama S T. *Catal Today*, 1992, 15: 179
- [3] Kojima R, Aika K. *Appl Catal A*, 2001, 219: 141
- [4] Rodriguez J A, Dvorak J, Jirsak T. *J Phys Chem B*, 2000, 104: 11515
- [5] Yu C C, Ramanathan S, Sherif F, Oyama S T. *J Phys Chem*, 1994, 98: 13038
- [6] Nagai M, Zahidul A M, Matsuda K. *Appl Catal A*, 2006, 313: 137
- [7] Keller V, Wehrer P, Garin F, Ducros R, Maire G. *J Catal*, 1995, 153: 9
- [8] Xiao T C, Hanif A, York A P E, Nishizaka Y, Green M L H. *Phys Chem Chem Phys*, 2002, 4: 4549
- [9] Ducreux O, Lynch J, Rebours B, Roy M, Chaumette P. *Stud Surf Sci Catal*, 1998, 119: 125
- [10] Xiong J M, Ding Y J, Wang T, Yan L, Chen W M, Zhu H J, Lu Y. *Catal Lett*, 2005, 102: 265
- [11] Jiao G P, Ding Y J, Zhu H J, Li X M, Li J W, Dong W D, Pei Y P. *Chin J Catal* (焦桂萍, 丁云杰, 朱何俊, 李显明, 李经纬, 董文达, 裴彦鹏. 催化学报), 2009, 30: 825
- [12] Jiao G P, Ding Y J, Zhu H J, Li X M, Dong W D, Li J W, Lü Y. *Chin J Catal* (焦桂萍, 丁云杰, 朱何俊, 李显明, 董文达, 李经纬, 吕元. 催化学报), 2009, 30: 92
- [13] Pei Y P, Ding Y J, Zang J, Song X G, Dong W D, Zhu H J, Wang T, Chen W M. *Chin J Catal* (裴彦鹏, 丁云杰, 臧娟, 宋宪根, 董文达, 朱何俊, 王涛, 陈维苗. 催化学报), 2012, 33: 808
- [14] Jiao G P, Ding Y J, Zhu H J, Li X M, Li J W, Lin R H, Dong W D, Gong L F, Pei Y P, Lu Y. *Appl Catal A*, 2009, 364: 137
- [15] Ding Y J, Zhu H J, Wang T, Jiao G P, Lü Y. US Patent 7 468 396. 2008
- [16] Ding Y J, Zhu H J, Wang T, Jiao G P, Lü Y. US Patent 7 670 985. 2010
- [17] Cvetanovic R J, Amenomiya Y. *Catal Rev-Sci Eng*, 1972, 6: 21
- [18] Volkova G G, Yurieva T M, Plyasova L M, Naumova M I, Zaikovskii V I. *J Mol Catal A*, 2000, 158: 389
- [19] Bahr H A, Jessen V. *Ber Deutsch Chem Ges*, 1930, 63: 2226
- [20] Kwon H, Thompson L T, Eng J Jr, Chen J G. *J Catal*, 2000, 190: 60
- [21] Neylon M K, Choi S, Kwon H, Curry K E, Thompson L T. *Appl Catal A*, 1999, 183: 253
- [22] Hofer L J E, Peebles W C. *J Phys Chem*, 1949, 53: 661
- [23] Yang S W, Li Y X, Ji C X, Li C, Xin Q. *J Catal*, 1998, 174: 34
- [24] Wang J, Castonguay M, Deng J, McBreen P H. *Surf Sci*, 1997, 374: 197
- [25] Hofer L J E, Peebles W C. *J Am Chem Soc*, 1947, 69: 893
- [26] Fujimoto K, Kameyama M, Kunugi T. *J Catal*, 1980, 61: 7

Co₂C上CO的程序升温脱附和程序升温表面反应研究

裴彦鹏^{a,c}, 丁云杰^{a,b,*}, 臧娟^{a,c}, 宋宪根^{a,c}, 董文达^{a,c}, 朱何俊^a, 王涛^a, 陈维苗^a

^a中国科学院大连化学物理研究所洁净能源国家实验室, 辽宁大连116023

^b中国科学院大连化学物理研究所催化基础国家重点实验室, 辽宁大连116023

^c中国科学院大学, 北京100049

摘要: 采用CO与金属Co在473 K反应400 h以上合成了Co₂C样品, 采用X射线衍射、透射电镜和CO程序升温还原对样品进行了表征, 并采用CO程序升温脱附和CO程序升温表面反应研究了Co₂C对CO的吸附及其加氢活化行为。结果表明, Co₂C微观结构由体相和表面钝化层两部分组成。表面钝化层可被CO于477 K左右去除。CO在Co₂C上有2个脱附峰, 其中低温脱附峰可能源于Co₂C上吸附的CO, 而高温脱附峰可能对应于残留于Co₂C晶格内的CO。Co₂C上吸附的CO可与H₂反应生成醇。

关键词: 碳化钴; 钝化层; 一氧化碳吸附; 加氢; 醇

收稿日期: 2013-04-07. 接受日期: 2013-05-10. 出版日期: 2013-08-20.

*通讯联系人. 电话/传真: (0411)84379143; 电子信箱: dyj@dicp.ac.cn

本文的英文电子版由Elsevier出版社在ScienceDirect上出版(<http://www.sciencedirect.com/science/journal/18722067>).

1. 前言

过渡金属碳化物自从被Levy和Boudart等^[1]报道具有类似Pt金属的催化性质以来一直备受关注. 研究发现, 过渡金属碳化物在加氢^[2], 合成氨^[3], 脱硫^[4], 脱氮^[5], 水汽变换反应^[6], 烷烃异构化^[7]和甲烷重整反应^[8]中表现出与贵金属接近或者相当的催化性能. 然而, 相关基础研究相对较少. Co_2C 一直以来被认为是费托合成催化剂失活的原因^[9,10]. 最近, 本课题组^[11,12]报道了活性炭负载的Co基催化剂上CO加氢生成 $\text{C}_1\text{--C}_{18}$ 线性混合伯醇可能与 Co_2C 的形成有关, 且Li和La等助剂可以调变该催化剂上 Co_2C 的生成量, 从而影响产物醇的选择性^[13–16].

程序升温脱附(TPD)和程序升温表面反应(TPSR)技术广泛应用于多相催化领域, 是研究表面吸附和表面反应的一种非常有效的方法, 能够为反应机理的探讨提供一些有力的证据^[17]. Volkov等^[18]认为, Co_2C 在CO加氢生成醇的反应中可以非解离吸附CO使其加氢生成醇, 但是有关 Co_2C 吸附CO的行为目前还没有报道. 采用TPD和TPSR技术研究CO在 Co_2C 上的吸附和反应行为, 对认识 Co_2C 在CO加氢合成醇反应中的作用有重要意义.

本文首先根据文献[19]合成出 Co_2C 样品, 采用X射线衍射(XRD)、高分辨透射电镜(HRTEM)和CO程序升温还原(CO-TPR)对其进行了表征, 再运用TPD和TPSR技术研究了CO在 Co_2C 上的吸附和反应行为, 并对反应机理予以探讨.

2. 实验部分

2.1. Co_2C 的制备

将10 g Co_3O_4 用 H_2 (60 ml/min)于523 K下还原4 h后, 降温至493 K, 切换成CO (60 ml/min), 维持468 h, 然后在CO气氛中淬火至室温, 最后于1% O_2/Ar (10 ml/min)中钝化2 h, 所得样品记为 $\text{Co}_2\text{C-A}$.

同上法制得样品 $\text{Co}_2\text{C-B}$, 只是将CO碳化时间延长至605 h.

2.2. 表征方法

XRD测试采用PANalytical公司X'Pert PRO型X射线衍射仪. $\text{Cu K}\alpha_1$ 光源, 电压40 kV, 电流40 mA, 扫描速度 $6^\circ/\text{min}$, 扫描范围 $2\theta = 30^\circ\text{--}60^\circ$.

HRTEM测试采用美国FEI公司Tecnai G2 F30型电子透射显微镜, 加速电压300 kV.

CO-TPR实验在美国Micromeritics公司Autochem 2910型化学吸附仪上进行. 样品(装填量200 mg)在CO

气流中(20 ml/min)以5 K/min从室温升温至573 K, 并保持1 h. 用瑞士OminiStar 300型质谱仪跟踪记录CO消耗和 CO_2 生成.

CO-TPD实验仪器和样品用量同上. 样品先在CO气流中以5 K/min升温至523 K处理1 h, 再切换成He恒温吹扫0.5 h. 然后在He气流中降至323 K, 吹扫40 min. 用脉冲进气法定量通入CO至吸附饱和, 用He气吹扫10 min后, 开始程序升温脱附, 用OminiStar 300型质谱仪跟踪记录脱附产物. 样品由323 K线性升温至1173 K, 升温速率5 K/min. 另取200 mg $\text{Co}_2\text{C-A}$ 样品于He气流下, 从室温以5 K/min升温至1173 K, 用OminiStar 300型质谱仪跟踪记录脱附产物, 所得结果作为空白实验.

TPSR实验仪器和样品用量同上. 样品预先在CO中以5 K/min升温至523 K处理1 h, 再切换成He恒温吹扫0.5 h, 然后在He气流中降至323 K吹扫40 min. 用脉冲进气法定量通入CO至吸附饱和, 用He气吹扫10 min后在10% H_2/Ar 气氛中以5 K/min升温至1000 K, 用OminiStar 300型质谱仪跟踪记录程序升温反应产物.

3. 结果与讨论

3.1. XRD和TEM结果

图1为 $\text{Co}_2\text{C-A}$ 和 $\text{Co}_2\text{C-B}$ 样品的XRD谱. 两种样品均于 37.0° , 41.3° , 42.5° , 45.7° 和 56.6° 处出现衍射峰, 可归属于 Co_2C (PDF 01-072-1369). 未观察到Co或者CoO的特征衍射峰, 说明这两种样品的体相已完全由 Co_2C 组成.

图2是 $\text{Co}_2\text{C-A}$ 样品的HRTEM照片. 从图2(a)中可以看出, 样品中心部分晶格条纹间距为 2.16 \AA , 与 Co_2C (PDF 01-072-1369)的(111)晶面间距相近. 由图2(b)可见, 所示的两组晶面的晶格条纹间距均为 2.46 \AA , 与CoO (PDF 00-009-0402)的(111)晶面间距相近. 结合样品的XRD分析结果, 可以认为所制样品微观结构由体相 Co_2C 和外表面CoO钝化层构成.

3.2. CO-TPR结果

过渡金属碳化物的表面钝化层对其反应及吸附性能会有影响, 因此在反应前一般需要予以去除^[20,21]. 我们采用CO程序升温还原方法考察了 $\text{Co}_2\text{C-A}$ 在CO气氛中钝化层的还原行为, 结果如图3所示. 可以看到, 随着温度的升高, CO出现一个消耗峰, 同时出现一个 CO_2 生成峰, 说明 Co_2C 的钝化层可以被CO还原.

3.3. CO-TPD结果

图4(a)是 $\text{Co}_2\text{C-A}$ 和 $\text{Co}_2\text{C-B}$ 样品的CO-TPD谱. 由图可见, 所有样品上均有2个CO脱附峰, 峰形相似. 将

Co₂C-A和Co₂C-B样品上处在较低温度的CO脱附峰分别记为A_L和B_L, 将在较高温度的脱附峰记为A_H和B_H. 显然, A_L与B_L的中心温度均为631 K, 而A_H的中心温度高于B_H的中心温度; A_L和A_H的峰面积均小于对应的B_L和B_H. 研究发现^[22], 573 K以上Co₂C分解需要时间较长, 而632 K以上则分解很快. 由此, 我们将A_L和B_L归属为Co₂C上的CO脱附峰, 而将A_H和B_H归因于Co₂C分解后的其它来源. 在碳化物(氮化物)合成中, 碳分子(氮分子)会以分子或者解离的形式残留在碳化物(氮化物)晶格中^[23,24]. 还可以看出, 随着碳化时间的延长, Co₂C晶格中碳含量可能愈加趋于饱和(Co₂C的晶格碳含量最大值9.24%), 从而导致吸附CO的表面活性位增多, 因而CO脱附峰面积增加. 同时, 由于碳化时间的延长, 残留在Co₂C晶格内的CO也更多. 但是, A_H与B_H的中心温度不同, 说明这种残留的CO的脱附温度可能受到晶格碳含量的影响.

采用CO-TPD技术考察了Co₂C-A样品在惰性气氛下未吸附CO的脱附行为, 结果如图4(b)所示. 可以看出, 在高温区(中心温度768 K)仍有CO的脱附峰, 与A_H和B_H的出现相吻合. 上文提到Co₂C在高温区不稳定, 这表明高温脱附的物种来源于Co₂C晶格内残留的CO. 同时注意到, 在631 K仍然存在CO脱附峰, 说明CO可能以化学吸附的形式残留在Co₂C表面上^[23]. 另外, 在536 K出现一个新的CO脱附峰. 考虑到样品未经CO处理, 该峰很可能是由钝化层中某物种脱附造成的.

3.4. CO-TPSR结果

图5是吸附CO的Co₂C-A样品在H₂气氛中的TPSR谱. 可以看出, 该样品在477 K和703 K有2个耗氢峰, 同时有2个甲烷($m/e = 16$)生成峰. 研究发现^[19,25], Co₂C在一定温度的H₂气氛中很容易分解为甲烷和金属Co. 因此, 477 K的甲烷生成峰可归因于Co₂C的加氢分解, 而703 K的峰归属于残留CO的加氢. 还可以看到, 水的质谱信号($m/e = 18$)只在703 K出现, 未在477 K出现, 从而证实了以上推断. 另外, Co₂C在TPSR过程中有甲醇($m/e = 31$)生成, 且生成发生在Co₂C尚未完全分解之前, 表明Co₂C本身能够使吸附的CO加氢生成甲醇. 在Co基催化剂上CO-TPSR实验中, 甲烷生成温度代表了Co解离CO的能力^[14,26], 而本文中在较低温度生成的甲烷来源于Co₂C的分解, 而不是CO加氢, 因此, 可认为吸附在Co₂C上的CO与甲醇的生成有关.

4. 结论

采用传统的方法合成了Co₂C样品, 与其他常见过渡金属碳化物类似, Co₂C样品表面存在着钝化层, 且可被碳源气体CO于477 K左右还原. Co₂C能吸附CO, 并可与H₂反应生成醇. 这表明Co₂C是Co基催化剂上合成醇的活性中心, 使其可能成为潜在的合成气制混合醇催化材料. 由于TPSR实验中甲醇的生成发生在Co₂C分解过程中, 因此仍不能排除醇在金属Co上生成的可能, 相关工作正在展开.